International Journal of Smart Home
Vol. 9, No. 12, (2015), pp. 75-80
http://dx.doi.org/10.14257/ijsh.2015.9.12.08

Effect of Discharge Location on Temperature Distribution during Electrical Discharge Machining

Baocheng Xie, Yanwen Zhang, Yuan Zhang, Ye Dai and Xianli Liu

School of Mechanical and Power Engineering, Harbin University of Science and Technology, Harbin, Heilongjiang Province 150080, China
xiebaocheng@hrbust.edu.cn

Abstract

The temperature field distribution has a dominant influence on machining efficiency and surface quality during electrical discharge machining (EDM). The discharge location is strongly related to temperature field distribution. Thus, the effect of discharge location on temperature distribution during EDM process should be illustrated to understand the mechanism of temperature field distribution. In this study, the thermal model for EDM process is established using ANSYS software to investigate the temperature field distribution. The model considers more realistic factors such as Gaussian distribution of heat flux, plasma channel radius, latent heat of melting, etc., to agree with actual machining situation. Numerical simulation analysis of the temperature distribution of the two consecutive spark discharges has been carried out considering the relative position relation of discharge location. Based on the numerical simulation, the effect of discharge location on the temperature distribution and material removal volume in pulse discharge process has been analyzed in detail.

Keywords*: Electrical discharge machining (EDM), Numerical simulation, Discharge location, Temperature distribution*

1. Introduction

Electrical discharge machining (EDM) is a non-contact machining method used widely in manufacturing dies and molds, etc., utilizing the intense heat generated by pulse discharge to melt and vaporize the local electrically conductive materials. Thousands of the erosive craters are created by the intense heat on the surface of the workpiece, producing the machined surface during the EDM process. Therefore, the temperature field distribution on the surface of workpiece has a dominant influence on material removal rate in EDM.

To investigate the temperature field distribution in EDM process, many efforts have been made in the past through simulation and experiment. For example, in [1-2], many different attempts for illustrating the temperature field distribution of single pulse discharge were made. Liu [3] reported that melt and vaporization were the primary removal way of insulating Al_2O_3 ceramic in single pulse discharge. Shabgard[4] simulated the temperature distribution on the surface of workpiece during a single discharge and assessed the effects of discharge parameters on machining efficiency and the recast layer thickness. Ming[5] proposed a hybrid intelligent process model based on finite-element method and Gaussian process regression to predict material removal rate and surface roughness. Weingartner[6] evaluated that the influence of high-speed rotating workpieces on tool wear in WEDM. Chen[7] established a thermo-numerical model of single pulse discharge to predict tool wear and material removal in micro-EDM of molybdenum. These mentioned models were performed to predict the temperature field distribution in EDM process. However, these studies are limited to a single discharge process, which

ISSN: 1975-4094 IJSH

cannot consider the effect of discharge location on temperature distribution and material removal during EDM process.

In the current study, a thermal model of EDM process was established to investigate the temperature field distribution. The more realistic factors such as Gaussian distribution of heat flux, plasma channel radius, latent heat of melting, etc., were considered to investigate the temperature field distribution. In addition, the effect of the relative position relation of discharge location on temperature distribution and material removal in pulse discharge process was discussed in detail

2. Mathematical basis of the Thermal Model

In EDM process, the intense heat generated in the plasma channel is transferred on the surface of workpiece and tool that results in material removal. Based on this characteristic of EDM, the material removal process is assumed as the heat conduction process. To simplify the numerical calculation, the following assumptions are considered:

1. The workpiece material is homogeneous and isotropic.
2. Only one discharge channel occurs in a single discharge, and the shape of discharge channel is cylindrical
3. The radiation heat dissipated into surrounding is negligible.

Fourier heat conduction equation (Eq.(1)) with boundary conditions is adopted as the governing partial differential equation, governing the transient temperature distribution in a cylindrical coordinate system:

$$\frac{c\rho}{\lambda}\frac{\partial T}{\partial t}=\frac{\partial^2 T}{\partial r^2}+\frac{1}{r}\frac{\partial T}{\partial r}+\frac{\partial^2 T}{\partial z^2} \tag{1}$$

Where r and z are the coordinates of cylindrical domain, T is temperature, ρ is the material density of the material, c is the specific heat of the material, λ is the thermal conductivity and t is the time. The associated initial and boundary conditions for the above governing partial differential equations are initial condition: for $t = 0$, $T = T_0$, T_0 is the room temperature, 25℃, the subsequent heat transfer process of a single discharge will be accumulated in the initial temperature distribution. As is shown in figure 1, the Gaussian heat flux distribution of the plasma channel is applied on the top surface F1 up to plasma channel radius $R(t)$. On the remaining region of the top surface F1, the cooling effect takes place in the way of the convection heat transfer. Since the side and bottom surface F2 and F3 are far from the plasma channel, no heat transfer conditions have been taken into account.

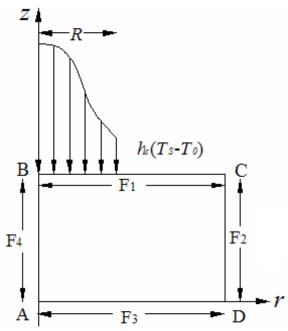

Figure 1. An Axisymmetric Thermal Model for the EDM Process

When the temperature field distribution in EDM process is solved, three characteristic parameters of the plasma channel should be presented. They are the plasma channel radius, the shape of heat flux and energy distribution factor. Many attempts have been made on the evolution of the plasma channel radius. The empirical equations have been presented to calculate the plasma channel radius [8-9]. Compared to other approaches, the equivalent heat input radius based on experimental data has been proposed by Ikai[9], which is closer to the actual EDM process. The plasma channel radius $R(t)$ (μm) as a function of the discharge duration t (μs) and the peak current I (A) are assumed as follows:

$$R(t) = 2040 \times I^{0.43} t^{0.44} \tag{2}$$

The second factor is the shape of heat flux loaded on the workpiece surface. There are several shapes of the heat source used in the previous work, such as a point shape, a uniform disk shape and Gaussian distribution shape. The associated Gaussian distribution of heat flux is more applicable to the actual EDM process. In the domain, the associated Gaussian distribution of heat flux for a single discharge has been adopted as follows [10]:

$$q(r) = \frac{4.45\eta UI}{\pi R(t)} \exp\left(\frac{-4.5r^2}{R(t)^2}\right) \tag{3}$$

Where η is the percentage of discharge energy transferred to the workpiece, namely energy distribution factor; U is the discharge voltage. Energy distribution factor η is another important factor in the model, governing the percentage of the total heat input from the plasma discharge channel. The different values of energy distribution factor were proposed by many researchers [2,5,7,11], ranging from 0.18-0.45. Comparing the experimental and analytical results, the constant value of η (0.3) has been adopted to estimate the temperature distribution in the model.

Due to the temperature of the plasma channel up to 10000K, the local material is heated above the melting points. The intense heat causes a phase change of material. Thus, the effect of latent heat on the temperature distribution is considered to make the model more realistic and reliable. Therefore, specific heat of phase change is dealt by enthalpy. The energy required to melt and vaporize the material per unit volume is estimated by using Eq. (4) and Eq. (5):

$$H_m = \int_{T_0}^{T_m} \rho c(T)\mathrm{d}T + \rho L_m \quad T_m \le T < T_v \tag{4}$$

$$H_v = \int_{T_0}^{T_v} \rho c(T)\mathrm{d}T + \rho L_m + \rho L_v \quad T_v \le T \tag{5}$$

Where $c(T)$ is the specific heat of workpiece, L_m and L_v are the latent heat of melt and vaporization, H_m and H_v are the total absorbed heat of melt and vaporization.

3. Results and Discussion

3.1. The Choice of Discharge Location

In EDM process, the erosive craters generated by the successive pulse discharges randomly disperse on the surface of workpiece. The superposition distribution of craters produces the “EDMed” surface, which affects the material removal rate and surface roughness. The relative position distribution of discharge location has a significant effect on the superposition distribution of craters in pulse discharge process. Thus, it is necessary to illustrate the effect of discharge location on mechanism of temperature distribution and material removal.

In single pulse discharge process, the shape of the crater in numerical simulation process is like a shallow bowl. Thus, the relative position relation of craters generated by the two consecutive spark discharges is divided into three cases: intersection, tangency and separation of two craters. The initial discharge location is adopted at the center of the surface region, and the second discharge location is decide based on three different relative positions, which is far away from the initial discharge location at a radius of crater, as is shown in figure 2.

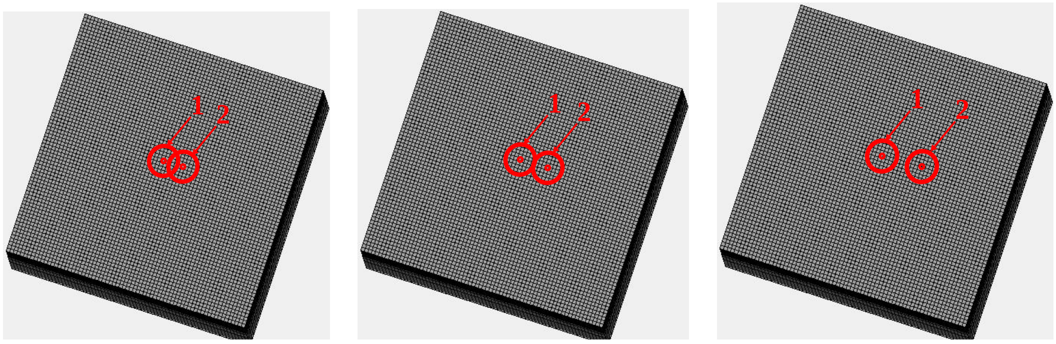

a) Intersection of Two Craters b) Tangency of Two Craters c) Separation of Two Craters

Figure 2. Choice of Discharge Location

3.2 Simulation Results and Discussion

In numerical simulation process, the discharge location was adopted as the center of plasma pulse channel and Gaussian distribution of heat flux. The initial discharge location was a fixed position, and the second discharge location was decided based on the relative position relation of discharge locations. The initial plasma channel radius $R(t)$ and Gaussian distribution of heat flux $q(r)$ was calculated by Eq.(1) and Eq.(2). Gaussian distribution of heat flux $q(r)$ is performed on the workpiece surface within the plasma channel radius $R(t)$, and the convection is applied on the surface notes outside the plasma channel radius $R(t)$. The model was solved based on the characteristic parameters of the plasma channel, such as the plasma channel radius, the shape of heat flux, latent heat of phase change and energy distribution factor. When the initial discharge has been calculated, the local material with the temperature value above the erosive temperature is removed from the workpiece surface. The crater is generated and the model is updated. Then the updated model and residual temperature field was calculated in the way of convection during pulse interval time. Finally, the second discharge of the different choice of discharge location was carried out.

The numerical simulations of temperature field distribution for the different cases with the current of 1.2A and the discharge duration of 2μs were carried out and the temperature field distribution contours were shown in figure 3. Figure 3 (a) shows the temperature field distribution of the initial discharge. Figure 3 (b)-(d) shows the temperature field distribution of the different relative position relation of two consecutive spark discharges. It can be seen that the maximum temperature of single pulse discharge varies with the different relative position of discharge position. It is because that the different relative position of discharge position results in the effective heating surface area. Due to Gaussian distribution of heat flux, plasma channel radius and discharge duration are constant, effective heating surface area plays an important role in temperature field distribution in the thermal model.

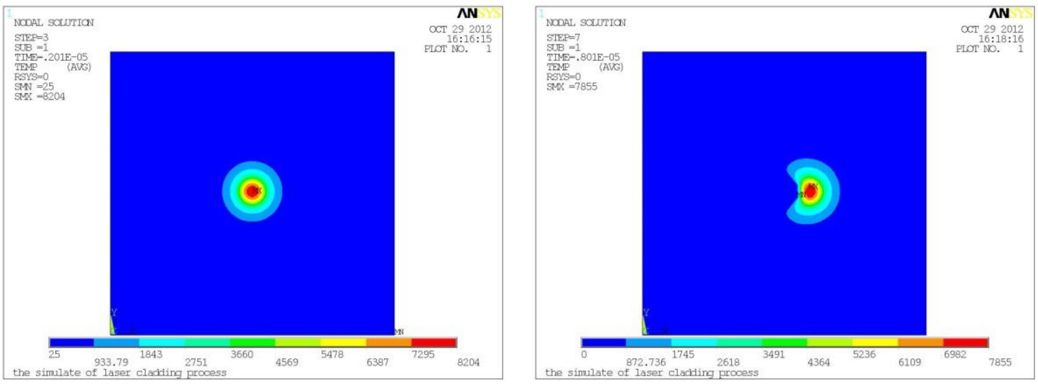

a) Initial of Discharge Position b) Intersection of Discharge Position

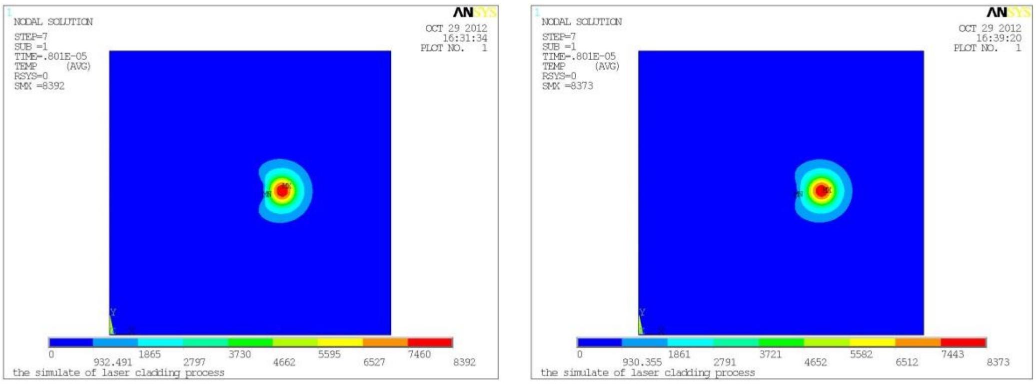

c) Tangency of Discharge Position d) Separation of Discharge Position

Figure 3. Temperature field distribution of different discharge position

When the single pulse discharge has been calculated, the local material with temperature value above the erosive temperature was selected and removed from the workpiece surface. Based on the temperature field distribution, the simulative crater can be obtained in each pulse discharge. The simulative craters for the different cases were achieved shown in figure 4. Figure 4 (a) shows the simulative crater of the initial discharge. Figure 4 (b)-(d) shows the simulative craters of the different relative position relation of two consecutive spark discharges.

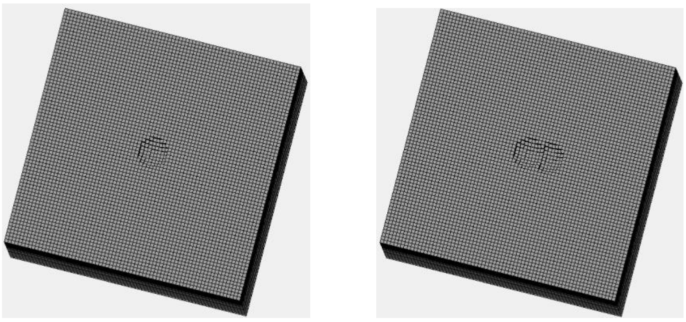

a) Initial of Discharge Position b) Intersection of Discharge Position

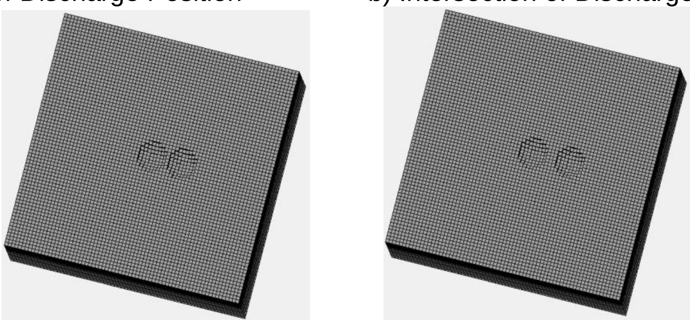

c) Tangency of Discharge Position d) Separation of Discharge Position

Figure 4. Schematic Diagram of Crater in Different Discharge Position

The simulative results of maximum temperature and crater volume by comparison were shown in the table 1. It is shown that the maximum temperature of tangency of discharge position is the highest, and those of intersection of discharge position is lowest. It is because that the effective heating surface area and the residual temperature field play an important role in temperature field distribution in the thermal model under the same discharge conditions, such as Gaussian distribution of heat flux, plasma channel radius and discharge duration.

Table 1. Temperature and Crater Volume in Different Discharge Position

	Maximum temperature(℃)	Crater volume(μm^3)
Initial of discharge position	8204	192
Intersection of discharge position	7835	162
Tangency of discharge position	8392	199
Separation of discharge position	8373	194

In the tangency of discharge position of the two consecutive spark discharges, the effective heating surface area is the whole region and the value of residual temperature field is higher than those in the initial temperature field. While in the separation of discharge position of the two consecutive spark discharges, the effective heating surface area is the same, and the value of residual temperature field is lower than those in the tangency of discharge position. Moreover, the effective heating surface area is the incomplete region, so the maximum temperature of intersection of discharge position is the lowest. The crater volume increased with the increasing of maximum temperature in the single pulse discharge. So the crater volume in the tangency of discharge position is the highest and the crater volume in the intersection of discharge position is the lowest, as is shown in the table 1.

4. Conclusions

In current study, the effect of discharge location on the temperature distribution during the two consecutive spark discharges in EDM process were analyzed based on the numerical simulation. The following main conclusions were drawn:

(1) Based on the relative position relation of discharge location, the temperature field distribution of single pulse discharge was carried out. The effect of discharge location on the temperature field distribution of the two consecutive spark discharges in EDM process has been investigated.

(2) In EDM process, the effective heating surface area and residual temperature field determine the temperature field distribution and material removal volume.

Acknowledgment

This research is sponsored by the national natural science foundation of China project (51375125 and 51505109) and Natural Science Foundation of Heilongjiang Province of China (E201440).

References

[1] S. H. Yeo, W. Kurnia and P. C. Tan, J Mater Process Tech., vol. 203, no. 1, **(2008)**, pp. 241-251.
[2] K. Salonitis, A. Stournaras, P. Stavropoulos and G. Chryssolouris, Int Journal of Adv Manuf Technol., vol. 40, no. 3-4, **(2009)**, pp. 316-323.
[3] Y. H. Liu, L. L. Yu, Y. L. Xu, R. J. Ji, Q. Y. Li, Y. H. Liu, L. L. Yu and Y. L. Xu, P I Mech Eng, B-Journal of Eng., vol. 223, no. 1, **(2009)**, pp. 55-62.
[4] M. Shabgard, R. Ahmadi, M. Seyedzavvar, S. N. B. Oliaei, M. Shabgard, R. Ahmadi and M. Seyedzavvar, Int Journal of Mach Tool Manu., vol. 65, no. 2, **(2013)**, pp. 79-87.
[5] W. Ming, G. Zhang, H. Li, J. Guo, Z. Zhang and Y. Huang, Int Journal of Adv Manuf Technol., vol. 74, no. 9-12, **(2014)**, pp. 1197-1211.
[6] E. Weingartner, K. Wegener and K. Friedrich, J Mater Process Tech., vol. 212, no. 6, **(2012)**, pp. 1298-1304.
[7] P. Allen and X. Chen, "Process simulation of micro electro-discharge machining on molybdenum", Journal Mater Process Tech., vol. 186, **(2007)**, pp. 346–355.
[8] K. Salonitis, A. Stournaras, P. Stavropoulos and G. Chryssolouris, Int J. Adv Manuf Technol., vol. 40, no. 3-4, **(2009)**, pp. 316-323.
[9] T. Ikai and K. Hashigushi, "Heat input for crater formation in EDM", Proceedings of international symposium for electro-machining_ISEM XI, EPFL, **(1995)**; Kyoto, Japan
[10] A. Descoeudres, C. Hollenstein, G. Wolder and R. Perez, Journal of Phys D Appl Phys., vol. 38, **(2005)**.
[11] H. Singh, Int J Heat Mass Tran, vol. 55, **(2012)**, pp. 5053-5064.

